Axon guidance genes identified in a large-scale RNAi screen using the RNAi-hypersensitive *Caenorhabditis elegans* strain *nre-1(hd20) lin-15b(hd126)*

Caroline Schmitz, Parag Kinge*, and Harald Hutter†

Max Planck Institute for Medical Research, Jahnstrasse 29, 69120 Heidelberg, Germany

Edited by Cornelia I. Bargmann, The Rockefeller University, New York, NY, and approved November 13, 2006 (received for review December 6, 2005)

The navigation of axons toward their targets is a highly dynamic and precisely regulated process during nervous system development. The molecular basis of this navigation process is only partly understood. In *Caenorhabditis elegans*, we isolated the RNAi-hypersensitive strain *nre-1(hd20) lin-15b(hd126)*, which allows us to phenocopy axon guidance defects of known genes by feeding RNAi. We used this mutant strain to systematically screen 4,577 genes on chromosomes I and III for axon guidance phenotypes. We identified 93 genes whose down-regulation led to penetrant ventral cord fasciculation defects or motoneuron commissure outgrowth defects. These genes encode various classes of proteins, ranging from secreted or putative cell surface proteins to transcription factors controlling gene expression. A majority of the genes is evolutionary conserved and previously uncharacterized. In addition, we found axon guidance functions for known genes like *pry-1*, a component of the Wnt-signaling pathway, and *ced-1*, a receptor required for the engulfment of neurons undergoing apoptosis during development. Our screen provides insights into molecular pathways operating during the generation of neuronal circuits and provides a basis for a more detailed analysis of gene networks regulating axon navigation.

Wnt | neuron | development | axon navigation

Directed outgrowth of neuronal processes like axons and dendrites reflects a complex navigational problem because of the large number of neurons involved in this process. Several conserved signaling systems have been described that influence the direction of outgrowth of navigating axons (for reviews, see refs. 1–3). Despite this progress in the identification of axon guidance signals, their small number does not match the complexity of the guidance process and the large number of neurons involved. The rather limited defects in mutants of known guidance cues indicate that a substantial fraction of axon guidance genes remains to be identified.

The nematode *Caenorhabditis elegans* is a suitable model for such a purpose, not only because its nervous system is simple and well described, but also because large-scale screens can be performed fast and easily. *C. elegans* has a comparatively small nervous system, with exactly 302 neurons in the adult hermaphrodite (4, 5). Axons and dendrites are typically unbranched and grow out in a stereotypic fashion. Because it is now possible to label neurons *in vivo* using fluorescent proteins like GFP (6, 7), large-scale direct visual screens for axon navigation defects have become feasible. In the last few years, RNAi in *C. elegans* (8) has become a powerful method to identify genes controlling particular biological processes, such as longevity, fat regulation, genome stability, RNAi, or transposon silencing (9). Unfortunately, RNAi, by feeding, does not function efficiently in the nervous system (10), effectively preventing use of this tool for the molecular analysis of axon guidance. Here we report the isolation of a strain in *C. elegans* that shows enhanced RNAi in the nervous system and the use of this RNAi hypersensitive strain for identification of genes regulating axon guidance.

Results

Isolation of an RNAi-Sensitive *C. elegans* Strain. To identify RNAi-hypersensitive mutants suitable for analysis of axon navigation, we performed a genetic screen with a transgenic *C. elegans* strain expressing GFP at moderate levels in the entire nervous system (*unc-119*::*GFP*). In a WT background, this strain showed no reduction of GFP expression in neurons after feeding of bacteria expressing GFP dsRNA (= feeding RNAi) (Fig. 1*c*). We screened for mutants with decreased neuronal GFP expression after feeding RNAi against GFP and identified a mutant we named *nre-1(hd20)* for neuronal RNAi efficient. In feeding RNAi experiments with *nre-1(hd20)*, typically only a small and variable number of neurons continued to express GFP at low levels (Fig. 1*d*). *Nre-1(hd20)* mutant animals are further characterized by a reduced number of progeny at 20°C (159 ± 18, $n = 4$) compared with WT (270 ± 18, $n = 4$). At 25°C, brood size is reduced even further to 7 ± 2 ($n = 10$) compared with 169 ± 10 in WT ($n = 4$). *Nre-1(hd20)* was mapped to the right arm of the X chromosome to a region containing the *lin-15b* gene, which was recently described to be RNAi hypersensitive (11). Sequencing of the *lin-15b* locus in our hypersensitive strain revealed a G to A transition in the splice acceptor site of the fifth intron (position 2463 of cosmid ZK678; GenBank accession no. Z79605). Destruction of this splice acceptor most likely leads to splicing out of the sixth exon, causing a frame shift. This effectively truncates the protein and eliminates the DNA-binding domains, suggesting that our strain contains a strong loss-of-function mutation in *lin-15b*. Our strain, however, has additional phenotypes, such as the sterility at 25°C, that are not shared by *lin-15* alleles. In fact, *lin-15ab(n765ts)* complements this sterility phenotype of *nre-1(hd20)*. We therefore conclude that our RNAi-hypersensitive strain contains two closely linked mutations, one of them in *lin-15b* and a second in a nearby gene. All of the phenotypes cosegregated in all genetic experiments, and we were never able to separate the different phenotypes in our strain. Most importantly, both mutations contribute to RNAi hypersensitivity, because our *nre-1(hd20) lin-15b(hd126)* strain is more effective than *lin-15b(n744)*, particularly in RNAi experiments targeting neuronally expressed genes (Table 1). Further, comparison with other RNAi-hypersensitive strains like *rrf-3*, *eri-1*, and an *eri-1; lin-15b* double mutant indicates that our *nre-1(hd20) lin-15b(hd126)* strain is the only one where known axon guidance genes can be phenocopied with high penetrance (Table 1; RNAi directed against *unc-40* or *unc-73*), making it the strain of choice for an RNAi screen for axon guidance genes.

Author contributions: C.S. and P.K. contributed equally to this work; H.H. designed research; C.S. and P.K. performed research; C.S., P.K., and H.H. analyzed data; and C.S. and H.H. wrote the paper.

The authors declare no conflict of interest.

This article is a PNAS direct submission.

Abbreviation: YFP, yellow fluorescent protein.

*Present address: National Chemical Laboratory, Dr. Homi Bhabha Road, Pune 411008, India.

†To whom correspondence should be addressed at the present address: Simon Fraser University, Burnaby, BC, Canada V5A 1S6. E-mail: hutter@sfu.ca.

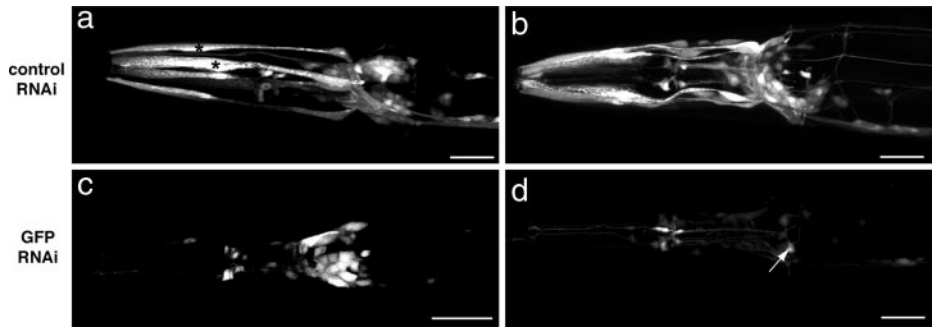

Fig. 1. Effectiveness of RNAi in neurons in *nre-1(hd20) lin-15b(hd126)* mutants. (*a*) *unc-119*::*GFP* is expressed in nonneuronal cells (asterisks) and neurons. Feeding of an empty RNAi vector does not affect GFP expression. (*c*) WT animals fed with a GFP RNAi vector (L4417): GFP expression is decreased in nonneuronal cells but not in neurons. (*b*) Feeding the control vector to *nre-1(hd20) lin-15b(hd126)* mutant animals does not affect GFP expression. (*d*) Feeding the GFP RNAi vector to *nre-1(hd20) lin-15b(hd126)* mutant animals leads to down-regulation of GFP expression in all cells. Only few neurons are left that weakly express GFP (arrow). Anterior to the left. (Scale bars, 20 μm.)

Large-Scale RNAi Screens for Axon Guidance Genes. We used *nre-1(hd20) lin-15b(hd126)* in a large-scale screen for axon guidance genes on chromosomes I and III. A fluorescent reporter was used to label interneurons of the motor circuit, as well as several classes of motoneurons (DA, DB, DD, and VD). This allowed analysis of the majority of axons in the ventral and dorsal cord, as well as outgrowth and navigation of motoneuron commissures that connect ventral and dorsal cord (Fig. 2 *a* and *e*). Feeding of 4,577 RNAi clones led to the identification of 93 genes with reproducible axon guidance phenotypes. Most prominent were defects in motoneuron commissure navigation, where commissures fail to reach the dorsal cord and extend in various lateral positions instead. Frequently, this was combined with abnormal branching and dorsal cord defaciculation [Table 2 (Com); Fig. 2 *f–h*]. Another common defect was abnormal midline crossing of ventral cord axons [Table 2 (VNC); Fig. 2 *b* and *d*]. Seventy-six different RNAi clones led to defects where motor- and/or interneuron axons crossed over into the left ventral cord axon tract either once or multiple times (Table 2). In one case, we found gaps in the dorsal cord or more rarely in the ventral cord (Table 2; Fig. 2*c*), indicating a failure of the outgrowth process *per se* rather than a navigation error. To analyze the defects in more detail, we labeled subsets of neurons with different fluorescent proteins, namely the excitatory DA/DB type motoneurons with cyan fluorescent protein and interneurons with DsRed and DD/VD motoneurons with yellow fluorescent protein (YFP). The majority of commissure as well as ventral cord defects are found in DD/VD motoneurons (Table 2). Ventral cord crossover defects in DD/VD motoneuron axons are found in 42 of the 93 RNAi clones, with 25 also sharing interneuron axon crossover defects and 8 both interneuron and DA/DB motoneuron crossover defects. Only three clones led to defects exclusively in interneurons, and no clone was found to interfere only with DA/DB axon guidance in the ventral cord.

To determine whether the identified genes govern axon guidance in other neuron populations, we repeated the RNAi feeding experiments with the positive clones isolated in the first screen and scored PVP and PVQ axons in the ventral cord using a different reporter strain. A total of 12 genes showed defects in PVPR and PVQL axon guidance with a penetrance ranging from 20% to 43% (Table 2, PVQ).

The axon guidance genes identified fall into distinct functional categories. A number of genes encode putative secreted or cell surface proteins like *cdh-4*, a member of the cadherin family of adhesion molecules (Table 2, Secreted or cell surface). *Cdh-4(RNAi)* leads to midline crossing defects within the ventral cord and defasciculation of the dorsal cord, suggesting that *cdh-4* plays a role in the adhesion of axons extending together in the same axon tract. *Ced-1(RNAi)* also leads to midline crossing and commissure navigation defects. The second category of genes contains signaling molecules that may connect signal–receptor complexes to effectors acting on the cytoskeleton (Table 2, Signaling). RNAi against *pry-1*, a component of the Wnt-signaling pathway, leads to defects in dorsal and ventral cord fasciculation and commissure guidance defects. RNAi against *unc-101*, a clathrin adapter protein implicated in trafficking of olfactory receptors (12), leads to gaps in the ventral cord and commissure guidance defects. Other genes in this category include kinases and phosphatases, which currently cannot be placed in any of the known signaling pathways. A smaller group (Table 2, Cytoskeleton) consists of proteins directly associated with the cytoskeleton, like myosin and kinesin family members as well as *unc-70*/spectrin. Another group of genes encodes transcription factors and regulators of protein degradation (Table 2, Transcription, splicing, protein modification/degradation). Among them is *cnd-1*, a NeuroD homolog that determines motoneuron cell fate as well as aspects of terminal differentiation like directed axon outgrowth (13) and homeobox and T-box containing transcription factors. Targeted protein degradation after ubiquitinylation is another way of controlling protein activity. We identified *wwp-1*, an E3 ubiquitin ligase, leading to defects in all analyzed axon trajectories. As in previous RNAi screens, a number of genes involved in general cellular metabolic processes were identified as well (Table 2, Cell metabolism). Here the axon guidance phenotypes most likely are a secondary consequence of a disturbed cell metabolism. In many cases, these RNAi clones produced additional phenotypes like slow growth or even larval or embryonic arrest, indicating that this category includes genes with a lethal phenotype that might not be completely penetrant in the RNAi experiment. Finally, a large fraction of the genes encodes proteins with no recognizable domains, making a functional classification difficult (Table 2, Unknown function). Several are conserved genes like *Y106G6H.8*, which encodes a small membrane protein, possibly a member of a novel receptor family involved in axon guidance.

Table 1. Comparison of RNAi-hypersensitive strains

RNAi against*	Percentage of animals with phenotype in WT	*rrf-3*	*eri-1*	*lin-15b*†	*lin-15b; eri-1*†	*lin-15b nre-1*‡
GFP	0 ± 0	0 ± 0	1 ± 1	74 ± 7	97 ± 3	98 ± 3§¶
unc-40	0 ± 0	0 ± 0	5 ± 4	9 ± 2	29 ± 1	73 ± 15§¶
unc-73	14 ± 5	57 ± 10	10 ± 2	15 ± 3	35 ± 4	77 ± 13§¶
dpy-13‖	100 ± 0	100 ± 0	100 ± 0	100 ± 0	100 ± 0	100 ± 0
daf-2	7 ± 3	6 ± 2	8 ± 4	3 ± 3	18 ± 6	31 ± 10§¶
lin-1	7 ± 9	27 ± 15	39 ± 15	68 ± 11	87 ± 5	77 ± 12§¶

Numbers are mean ± SD for three independent experiments (n = 56–100 for each experiment with *lin-1, daf-2, dpy-13,* and GFP; n = 28–65 for *unc-40* and *unc-73*).

*Phenotypes scored: GFP expression in neurons scored with *rhls13 [unc-119*::*GFP]* (GFP); ventral cord defasciculation and commissure defects scored with hdls17 (*unc-40*, *unc-73*); Dpy (*dpy-13*); dauer formation (*daf-2*); multivulva (*lin-1*).

†*lin-15b (n744).*

‡*lin-15b (hd126).*

§Significant with $P < 0.01$ compared with WT (unpaired t test).

¶Significant with $P < 0.01$ compared with *lin-15b (n744)* (unpaired t test).

‖ Strains show different severity of dumpy phenotype: wt < *nre-1 lin-15b/lin-15b* < *rrf-3/eri-1/lin-15b; eri-1*.

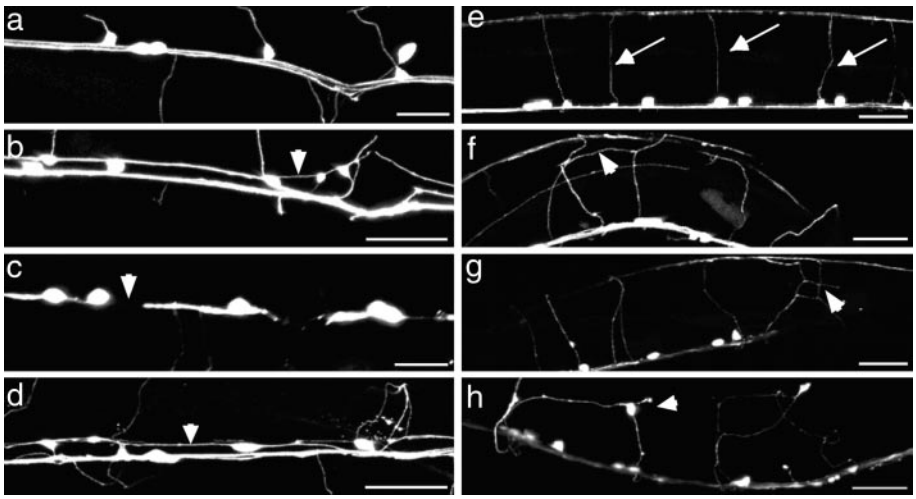

Fig. 2. Representative axon guidance phenotypes. (*b*, *c*, and *f*) Phenotypes generated by RNAi. (*g* and *h*) Phenotypes of genetic mutants. (*a*) WT: all GFP labeled axons run tightly fasciculated in the right tract. (*b*) *Cdh-4(RNAi)*: axons cross over into the left axon bundle (arrowhead). (*c*) *Unc-101(RNAi)*: gaps (arrowhead) indicate a premature stop of axon outgrowth. (*d*) *Pry-1(mu38)*: ventral cord midline crossing defects (arrowhead). (Scale bar, 20 μm.) Ventral view, anterior to the left. (*e*) WT: commissures grow circumferentially to the dorsal cord (arrows). (*f*) *F10G8.4(RNAi)*: premature branching of commissures (arrowheads). (*g*) *ced-1(e1735)*: abnormal branching of commissures (arrow). (*h*) *Unc-101(m1)*: lateral extending axons (arrowhead). (Scale bar, 20 μm.) Lateral view, ventral side down.

***Pry-1*, *ced-1*, and *unc-101* Mutants Show Axon Guidance Defects.** Genetic mutations are not available for most of the genes identified in our screen. However, we were able to test the axon guidance function of several genes identified in the screen by analyzing existing genetic mutants. In *lin-39* mutant animals, we could not observe any axon guidance defect, indicating that our collection contains some "false positives." By contrast, *pry-1*, *ced-1*, and *unc-101* mutants show axon outgrowth and/or navigation defects like the corresponding RNAi experiments (Fig. 2 *d*, *g–i* and Table 3). *Pry-1(mu38)* mutants showed the strongest defects, with branched commissures and ventral cord midline crossing defects (Fig. 2*d*). *Ced-1(e1735)* mutants exhibit only commissure defects (Fig. 2*g*), and *unc-101(m1)* mutants are characterized by branched lateral outgrowing commissures and prominent gaps, predominantly in the dorsal cord (Fig. 2 *h* and *i*). This shows that the RNAi phenotypes can be confirmed by the analysis of genetic mutants, which are more suitable for a detailed study of gene function.

Discussion

***Nre-1(hd20) lin-15b(hd126)* Is a Potent RNAi-Sensitive Mutant Combination.** Mutations affecting the RNAi response of cells have been identified. Mutations in genes abolishing the RNAi response have been instrumental in the identification and characterization of the molecular machinery mediating the effects of dsRNA in cells (14, 15). Delivering the dsRNA by feeding (the method of choice for high-throughput screens) does not work efficiently for neuronal genes. Mutations with increased sensitivity to dsRNA, like *rrf-3* (16) or *eri-1* (17), have been isolated but have not really solved this problem. Recently, it was shown that mutations in retinoblastoma pathway components, like *lin-15b* or *lin-35*/Rb, can enhance RNAi (11, 18). This pathway seems to act in parallel to the *eri-1*/*rrf-3* pathway, because a combination of mutations in those pathways is even more RNAi-hypersensitive than the single mutants (11, 18). A combination of *eri-1* and *lin-15b* was recently used successfully in an RNAi screen to identify genes affecting synaptic transmission (19). Although the *eri-1;lin-15b* mutant combination also allows to phenocopy axon guidance defects to a certain extent, we find that the *nre-1(hd20) lin-15(hd126)* mutant combination described here provides a better genetic background to screen for genes involved in axon guidance. One of the mutations in our strain, *nre-1(hd20)*, shares phenotypes with *eri-1* and *rrf-3*, like the temperature-sensitive decrease in brood size. *Nre-1* might be involved in RNA metabolism like *eri-1* [a 3′ exonuclease (17)] and *rrf-3* [a RNA-dependent RNA polymerase (16)], possibly interfering with the down-regulation of the RNAi response.

Genes Controlling Axon Navigation. Our screen identified most of the known axon guidance genes in *C. elegans* on the investigated chromosomes (i.e., *unc-40*, *unc-71*, *unc-73*, and *hse-5*). A few genes like *lin-11* or *unc-119* were missed, indicating that even in our highly sensitized background, it is not possible to identify the complete set of genes needed for axon navigation. We also identified a few genes (i.e., *lin-39*) as having a role in axon navigation, where gene mutations do not seem to confirm this function. One possible explanation for the discrepancy is a dependence of the RNAi effect on axon guidance on the particular genetic background used in the screen. *Lin-39* and *lin-15b*, which is mutated in the strain used in the RNAi screen, are both transcription factors and share a function in vulva cell fate specification (20). The RNAi experiments could point to a synergistic function of these genes in axon guidance.

The 93 genes affecting interneuron and/or motoneuron navigation fall into distinct functional categories, showing that our screening approach was able to identify genes at all levels of axon guidance regulation. One class of genes encodes putative secreted or cell surface proteins. One of those proteins (D1044.2) has structural similarity to nidogen (NID-1), a component of the basement membrane known to be important for the correct positioning of axon bundles in *C. elegans* (21). Another gene in this category is the cadherin CDH-4, one of two fat-like cadherins encoded in the *C. elegans* genome (22). No function for *cdh-4* has been described. We have isolated mutants, confirming the function for *cdh-4* in axon guidance (C.S. and H.H., unpublished results). Fat-like cadherins are expressed in the developing nervous system in vertebrates, and mice lacking mFat1 exhibit defects in forebrain and eye development (23, 24), suggesting an evolutionary conserved function for fat-like cadherins in nervous system development.

Midline crossing defects of interneuron and/or motoneuron axons in the ventral cord were a prominent phenotype in our RNAi screen. PVP and PVQ axons, which also run in the ventral cord, were rarely affected, leading to two conclusions. First, the majority of the genes identified has a specific role in the navigation of certain classes of axons rather than a general role in axon guidance affecting every neuron (as would a global signal). Second, different axons extending in the same axon bundle apparently use different combinations of signals to navigate and stay on course. This adds an additional level of complexity and hints at how neuronal circuits can be formed in a robust way: by using not a few globally acting signals but separate sets of signals for different groups of axons, even for those that travel along the same path. This confirms earlier studies, which suggested that different classes of neurons with axons in the ventral cord use different combinations of guidance signals to navigate (25). Conversely, particular guidance signals in the ventral cord apparently are shared by neurons belonging to the motor

Table 2. RNAi clones leading to axon guidance phenotypes

Gene (Chr)	Size, aa	Description	Conserved*	Com†	Com type	VNC‡	Axon type	DNC§	PVQ¶	Other phenotype‖
Secreted or cell surface (12 genes)										
unc-40 (I)	1,415	Netrin receptor, DCC homolog	Yes	+++	D	+++	I	++	−	Gro, Unc, Eg
unc-71 (III)	1,042	ADAM-type metalloprotease	Yes	++	D	+	D	+++	−	
ced-1 (I)	1,111**	EGF domain	Yes	+	D	++	D	−	−	
B0041.5 (I)	429	RhaT domain	Yes(d)	++	D	++		++	++	
nas-5 (I)	360	Astacin metalloprotease	Yes	++	D	+++		++	−	
C24G7.1 (I)	608	Sodium channel	Yes	++	D	++	D	++	−	
F44E2.4 (III)	1,283	LDL receptor domain	No	+++	A,D	−		−	−	
grl-22 (III)	162	Groundhog related	No	++	D	+		−	−	
cdh-4 (III)	4,307	FAT-like Cadherin	Yes	−		++	D,I	+	−	
C09D4.1 (I)	586**	AraJ domain	Yes	+	D	++	def	+	−	Unc
T23B3.4 (I)	395	Sulfakinin receptor	Yes	+	D	++	D,I	+	−	
D1044.2† (III)	1,090	Nidogen N terminus	Yes(d)	+	D	+		−	−	
Signaling (12 genes)										
pry-1 (I)	586	Axin homolog, Wnt signaling	Yes	++	D	++	D	+	−	Gro, Unc, Lvr
unc-73 (I)	2,488**	GNEF, Trio homolog	Yes	+++	D	++	A,D,I	++	−	Gro, Unc, Egl
unc-13 (I)	2,155**	C2, DUF1041 domains	Yes	+	D	+	D,I	−	++	Gro
unc-101 (I)	422	Clathrin adaptor protein AP1	Yes	+	D	++		−	−	
ZC581.9 (I)	827	S/T kinase	Yes	++		++++		+	−	
F10G8.4 (I)	395	Tyrosine phosphatase	Yes(d)	+++	D	+++	D,I	++	−	Gro
smd-1 (I)	368	SAM decarboxylase	Yes	++	D	+++	D,I	+	−	
F47B3.1 (I)	363	Tyrosine phosphatase	Yes	++	D	++	D,I	++	−	
pde-6 (I) (Y95B8A.10)	760	Phosphodiesterase	Yes	++	D	++	A,D,I	−	+	
F26E4.5 (I)	474	SH2 domain, tyrosine kinase	Yes	+	D	++	D,I	−	−	
ZC155.7 (III)	329	Syntaxin	Yes	++	D	+		−	−	
Y52D3.1 (III)	388	S/T kinase	Yes (d)	+	D	+		−	−	
Cytoskeleton (6 genes)										
unc-70# (V)	2,302**	β-Spectrin	Yes	++++	D	−		+	++	Jnc, Gro
nmy-2 (I)	2,003	Myosin heavy chain	Yes	++	D	+++	def	−	−	Gro
unc-95 (I)	350	LIM domain adaptor protein	No	+++	D	+++	D,I	++	−	Unc, Egl
lem-3 (I)	732	Ankyrin repeat, LEM domain	Yes (d)	++	D	+++	D,I	++	−	
hum-5† (III)	1,017**	Myosin heavy chain	Yes	++	D	−		−	−	
unc-116 (III)	815	Kinesin heavy chain	Yes	++	D	−		+	−	
Transcription, splicing, protein modification/degradation (15 genes)										
lin-59 (I)	1,312	ASH1/trithorax homolog	Yes (d)	+++	D	+++		++	−	Gro, Egl
sur-2 (I)	1,589**	CRSP3 homolog	Yes	++	D	+++	A,D,I	++	−	
ZK1128.5 (III)	446	Swp73/BAF60 homolog	Yes	++++	D	++	I	+++	−	
rnp-6 (I)	749**	HALF-PINT, (FIR)/PUF6 homolog	Yes	++	D	+++	D	++	++	Gro, Unc, Egl
hmg-3 (I)	689	SSRP1 homolog	Yes	+++	D	+++	D,I	++	−	Gro, Unc
tbx-9 (III)	292	T-box transcription factor	Yes	+++	A,D	−		+++	−	
F25D7.1 (I)	245	Derlin-1 homolog	Yes	+	D	++++		−	−	
lin-39 (III)	253	HoxD4/Dfd homolog	Yes	++++	D	−		−	++	
cnd-1 (III)	192	NeuroD homolog	Yes	+++	D	−		+	−	Egl
Y95B8A.7 (I)	608	zfr1 homolog	Yes	++	D	++	D,I	++	−	
wwp-1 (I) (Y65B4BR.4)	794**	WWP1 homolog	Yes	++	D	++	D,I	++	−	Unc
ZC328.2 (I)	386	Zinc finger TF	Yes(d)	+	D	++		−	−	
ceh-13 (III)	202	Hox1/labial homolog	Yes	+	D	++	A,D,I	+	++	
dpy-27 (III)	1,469	Condensin complex member	Yes	++	A,D	−		−	−	Dpy
hse-5 (III)	616	HS-C5-epimerase	Yes	+	D	−		−	−	
Cell metabolism (17 genes)										
cua-1 (III)	1,238	Copper transporter	Yes	++++	A,D	++++	def	++++	−	Unc, gro, Lvr
Y56A3A.21 (III)	159	TRAP-delta homolog	Yes	++++	D	++++		++	−	Unc, gro,
Y105E8B.9 (I)	628	β-Glucuronidase	Yes	++	D	+++		++	++	Gro
T05E8.3 (I)	856	DEAH-box RNA helicase	Yes	+		+++	D,I	++	−	Gro, Unc
Y105E8A.23 (I)	944	RNA polymerase	Yes	+	D	+++	def	++	−	Gro
T21G5.5 (I)	445**	KH1 domain (RNA binding)	Yes	++	D	+++		++	+	Unc, Egl

circuit. Ventral cord defects in DA/DB motoneurons are always, and defects in *glr-1*::*GFP* expressing interneurons are predominantly, found in combination with VD/DD defects, suggesting that the affected genes belong to an axon guidance pathway shared by these neurons.

Functions for *ced-1*, *unc-101*, and *pry-1* in Axon Navigation. To validate the screen results, we analyzed mutants of *ced-1*, *pry-1*, and *unc-101* and found axon guidance defects similar to those in the RNAi screen, suggesting that these genes have previously unrecognized functions in neuronal circuit formation. *Ced-1* is an EGF-domain-containing receptor implicated in cell–cell recognition between apoptotic and hypodermal cells destined to engulf them (26). *Ced-1* has been shown to be expressed in many neurons in the head and ventral cord (26). Our results show that the receptor has a second function in circumferential guidance of motoneuron commissures. *Unc-101* encodes a homolog of the medium chain of the clathrin adaptor complex AP1 (9, 27). Trafficking of olfactory receptors depends on *unc-101* (12), suggesting that in *unc-101* mutants, altered axon guidance receptor localization could be responsible for the observed defects. *Pry-1* encodes the *C. elegans* axin homolog (28). RNAi against *pry-1* leads to severe defects,

Table 2. continued

Gene (Chr)	Size, aa	Description	Conserved*	Com†	Com type	VNC‡	Axon type	DNC§	PVQ¶	Other phenotype‖
mdt-18 (I) (C55B7.9)	232	MED18 homolog	Yes	++	D	++	D,I	+	++	Gro, Unc
lpd-3 (I)	1,599	Lipid metabolism	Yes	++	D	++		++	−	
rpl-17 (I)	187**	Ribosomal L17 protein	Yes	++	D	++	D,I	+	−	Gro, Unc
F43G9.3 (I)	294	Mitochondrial carrier protein	Yes	++	D	+++		−	−	
E03H4.1 (I)	–	Transposase	-	++	D	++	A,D,I	+	−	
C41D11.2 (I)	365	Translation initiation factor 3	Yes	++	D	++	def	−	−	
mdt-21 (III)	132	Peptidase	Yes	++	D	+	A,D,I	+	−	Unc, Gro
lbp-5 (I)	136	H-FABP homolog	Yes	++	D	++	D	−	−	
W03D8.8 (I)	430	Acyl-CoA thioesterase	Yes	+	D	++	D	+	−	
dhs-9 (III)	319	Short-chain dehydrogenase	Yes	++	D	+	D,I	−	−	
Y37D8A.7 (III)	–	Transposase	−	++	D	−		−	−	
Unknown function (31 genes)										
Y106G6H.8 (I)	112	DUF423, TM	Yes	+++	D	+++		++	−	Gro
Y63D3A.9 (I)	277	F-box protein	No	++	D	+++	D,I	++	−	
T24D1.3 (I)	349	RING finger	No	++	D	++		++	+	
T07A5.2 (III)	301	UNC50 domain	Yes	+++	D	−		+	−	Unc, Lev
pqn-20 (I)	1,239	Poly-Q-containing protein	Yes(d)	+	D	++		+	−	
C38C10.3# (III)	301	DUF508	No	++	D	−		−	−	−
D2007.2 (III)	195	MSP domain	No	++	D	+		−	−	
T28A8.3 (III)	621	SPK domain	No	+	D	+	D,I	−	++	
F59A2.6 (III)	1,133	GRIP domain	Yes	+	D	−		−	−	
Y47G6A.29 (I)	2460	No known domains	Yes(d)	++	D	+++	A,D,I	++	−	
F46F11.9 (I)	1,282**	No known domains	Yes(d)	++	D	++		+++	−	Gro, Unc, Egl
C40H1.3 (III)	504	No known domains	Yes(d)	+	D	−		−	−	
K04H4.2 (III)	967**	No known domains	Yes(d)	+	D	−		−	−	Gro
Y34D9A.3 (I)	639	No known domains	No	+++	D	+++	D,I	++	−	Unc
Y48G1C.8 (I)	828	No known domains	No	+	D	+++	def	+++	−	Gro, Unc
F29D11.2 (I)	1,153	No known domains	No	++	A,D	+++	A,D,I	++	−	Unc, Dpy
F26B1.1 (I)	304	No known domains	No	++	D	+++	D	++	−	
C17F3.1 (I)	88	No known domains	No	+++	D	++	D,I	++		
Y55D5A. 1 (III)	285**	No known domains	No	++	D	++		+++	−	Egl
F48C1.4 (I)	104	No known domains	No	++	D	++	D	+	−	Dpy, Lvr
Y106G6A.5 (I)	210	No known domains	No	++	D	+++	D,I	−	−	
Y43F4B. 3 (III)	216	No known domains	No	+++	D	+		−	−	
Y106G6A.2 (I)	428	No known domains	No	+	D	+++	D,I	−	−	
ZK973.8 (I)	392	No known domains	No	+	D	+++	def	−	−	
Y18D10A.21 (I)	286	No known domains	No	−		+++		−	−	
Y37H9A.1 (I)	514**	No known domains	No	+	D	++	I	−	−	
T15D6.9 (I)	407	No known domains	No	+	D	++	D,I	++	−	
Y106G6A. 4 (I)	175	No known domains	No	++	D	++	D,I	+	−	
F54D8.6 (III)	783	No known domains	No	+	D	−		+	−	
T04C9.2 (III)	116	No known domains	No	+	D	+		−	−	
F54H12.2 (III)	419	No known domains	No	+	D	−	D,I	−	−	

Chr, chromosome; Com, commissure.

*Yes indicates BLAST scores higher than 1e-10 for >70% of the protein length. Yes(d) indicates BLAST scores higher than 1e-10 for >30% but <70% of the protein length. No indicates BLAST scores lower than 1e-10 and/or <30% protein length. Similar or homologous proteins found in other animals (BLAST search results evaluated).

†More than two commissures not reaching the dorsal cord (1% defects in WT); Comm type A, DA/DB motoneuron commissures have defects; Comm type D, DD/VD motoneuron commissures are affected. RNAi clone contained wrong insert (see *Materials and Methods*).

‡Midline crossing defects in the ventral nerve cord (VNC) (6% defects in WT); axon type A, DA/DB motoneuron axons in the ventral cord are affected; Axon type D, DD/VD motoneuron axons; axon type I, interneuron axons; def, overall defasciculation of the ventral cord.

§Dorsal nerve cord (DNC) defasciculation (6% defects in WT).

¶PVPR/PVQL guidance defects (midline crossing or outgrowth in the right axon tract 4% defects in WT). +, Defects <25% but significantly higher than in WT ($P < 0.01$, χ^2 test). ++, 25–49% animals with defects. +++, 50–74% animals with defects. ++++, 75–100% animals with defects.

‖Additional phenotypes observed: Dpy, dumpy; Egl, egg-laying defect; Gro, growth defect; Lev, levamisole resistant; Lvr, larval arrest; Unc, uncoordinated movement.

**Longest splice variant.

indicating that Wnts play a role in a variety of axon guidance decisions in *C. elegans*. Members of the Wnt family have been shown to control axon navigation in *Drosophila* as well as in mice (reviewed in refs. 29 and 30). An important role for Wnts in axonal navigation along the anterior–posterior axis was shown recently in *C. elegans* as well (31–33). We show here that a central component of the canonical Wnt signaling pathway, *pry-1,* is involved in left–right (within the ventral cord) and dorsoventral axon guidance decisions (commissures). It seems most likely that a combination of the above-mentioned Wnts is involved here as well, because RNAi against individual Wnts does not phenocopy the defects seen in *pry-1* (data not shown).

In summary, we isolated the RNAi-hypersensitive mutant combination *nre-1(hd20) lin-15b(hd126)* suitable for RNAi analysis of axon guidance. The large number of axon guidance genes identified in our screen provides a basis for further molecular analysis of directed axon outgrowth at all regulation levels, from extracellular signals to transcriptional control of axon guidance genes.

Materials and Methods

Nematode Strains and GFP Markers. For the RNAi screen, the following promoters were used to drive YFP expression in a subset of neurons with axons in the ventral cord: interneurons, *glr-1* (35,

Table 3. Axon guidance defects in *unc-101*, *ced-1*, and *pry-1* mutants

Genotype	Com*	VNC†	DNC‡	*n*
WT	6	2	0	111
unc-101 (m1)	26§	8	30§	106
ced-1 (e1735)	23§	6	4	129
pry-1 (mu38)	66§	42*	48§	65

Animals were examined with an extrachromosomal transgene *hdEx191[glr-1*::*YFP, unc-129*::*YFP, unc-47*::*YFP, rol-6(su1006)]* labeling motor- and interneurons.

*More than one commissure not reaching the dorsal cord.

†Midline crossing defects in the ventral nerve cord (VNC).

‡Dorsal nerve cord (DNC) defasciculation or gaps in the dorsal cord (*unc-101* only).

§Significant with $P < 0.01$ (χ^2 test). Com, commissure.

36); D-type motoneurons, *unc-47* (37); and DA/DB motoneurons, *unc-129* (38). The marker strain *hdIs17[glr-1*::*YFP, unc-47*::*YFP, unc-129*::*YFP, rol-6(su1006)]* was generated (originally for a different purpose) in a CB4856 background (Hawaii isolate). For the RNAi screen, *hdIs17* (three times outcrossed to Bristol N2) was crossed into *nre-1(hd20) lin-15b(hd126)* to obtain VH715: *hdIs17* I; *hdIs10[unc-129*::*CFP, glr-1*::*YFP, unc-47*::*DsRed, hsp-16*::*rol-6] V*; *nre-1(hd20) lin-15b(hd126)* X. The following mutations and markers also were used: Bristol N2, *rhIs13[unc-119*::*GFP; dpy-20(+)]* V; *hdIs26[odr-2*::*CFP, sra-6*::*DsRed2]* III; *hdIs32[glr- 1*::*DsRed2]* III*; rrf-3(pk1426)* X*; ced-1(e1735) I; unc-101(m1) I; pry-1(mn38) I,; eri-1(mg366)* IV; *lin-15(n744)* X; *eri-1(mg366)* IV; *lin-15(n744)* X. All strains were cultured at 20°C using standard methods.

Mutant Isolation. The *nre-1(hd20) lin-15b(hd126)* mutant strain was isolated after ethyl-methyl-sulfonate (EMS) mutagenesis (50 mM EMS for 4 h) of *rhIs13[unc-119*::*GFP; dpy-20(+)]* (panneuronal GFP expression). The F_1 and F_2 generations of the mutagenized animals were fed with the *E. coli* strain HT115(DE3) containing the RNAi feeding vector L4417 (Fire vector kit; Addgene, Cambridge, MA). *Nre-1(hd20) lin-15b(hd126)* was selected out of 20,000 genomes as having significantly reduced GFP expression in neurons. *Nre-1(hd20) lin-15b(hd126)* was mapped by using SNP after crossing with the strain CB4856 (Hawaii isolate). The sterility phenotype was used to identify *nre-1* homozygotes, which were then also tested for RNAi hypersensitivity. Both traits mapped to a region between SNP pkP6117 on cosmid C27C12 (corresponding to map position 21.4) and the end of the right arm of the X chromosome.

RNAi Screening and Analysis of Axonal Defects. RNAi by feeding was performed as described (39) with the following modifications: RNAi feeding clones were grown for 16 h in LB culture with 50 μg/ml ampicillin and seeded onto agar plates containing 1 mM isopropyl β-D-thiogalactoside and 50 μg/ml carbenicillin. Twenty-four hours later, L3 stage hermaphrodites were placed on the plates and incubated for 5 days at 20°C. Bacterial clones leading to axonal defects were retested twice, and only clones giving significant phenotypes with $P < 0.01$ (χ^2 test) in all three experiments were scored as positive. All inserts from positive clones were sequenced to confirm identity of the clone. The following discrepancies were detected: well for clone JA_C16C10.8 contained clone JA_T02C12.1, JA_D1044.1 contained JA_D1044.2, JA_C38C10.2 contained JA_C38C10.3, JA_B0280.4 insert corresponds to *unc-70*. For phenotypic analysis, worms were washed off the feeding plates with M9 buffer containing 3 mM levamisole and mounted on agar pads. Axon guidance defects were scored with a Zeiss Axioskop Microscope (Zeiss, Oberkochen, Germany) by using a 40× Plan Neofluar objective and a standard YFP filter set. Stacks of confocal images were recorded with a Leica (Deerfield, IL) TCS SP2 microscope and are shown as maximum-intensity projections generated by ImageJ software (http://rsb.info.nih.gov/ij).

Statistical Analysis. Significances of differences in defects between control strains and mutant strains/RNAi-treated animals were determined by χ^2 test. All axon guidance defects in Table 2 are significant, with $P < 0.01$ in comparison with the YFP marker strain in WT background.

We thank Andrew Fire (Stanford University, Stanford, CA) for vectors, the Ahringer laboratory (University of Cambridge, Cambridge, U.K.) for the RNAi library (obtained from Geneservice, Cambridge, U.K.), the Kaplan laboratory (Harvard University, Cambridge, MA) for the *eri-1(mg366)* IV; *lin-15(n744)* X strain, Suse Zobeley and Ilse Wunderlich for help with cloning and the generation of transgenic strains, and members of our laboratory for critical discussion of the experiments and comments on the manuscript. Some of the strains used in this work were obtained from the *Caenorhabditis* Genetics Center (University of Minnesota, Minneapolis, MN). This work was supported by the Max Planck Society, Deutsche Forschungsgemeinschaft Grants GRK 484 and GRK 791 and Canadian Institutes of Health Research Grant MOP77786 (to H.H.).

1. Araujo SJ, Tear G (2003) *Nat Rev Neurosci* 4:910–922.
2. Dickson BJ (2002) *Science* 298:1959–1964.
3. Yu TW, Bargmann CI (2001) *Nat Neurosci* 4(Suppl):1169–1176.
4. Sulston JE, Horvitz HR (1977) *Dev Biol* 56:110–156.
5. Sulston JE, Schierenberg E, White JG, Thomson JN (1983) *Dev Biol* 100:64–119.
6. Chalfie M, Tu Y, Euskirchen G, Ward WW, Prasher DC (1994) *Science* 263:802–805.
7. Hutter H (2004) *J Microsc* 215:213–218.
8. Timmons L, Fire A (1998) *Nature* 395:854.
9. Sugimoto A (2004) *Differentiation* 72:81–91.
10. Timmons L, Court DL, Fire A (2001) *Gene* 263:103–112.
11. Wang D, Kennedy S, Conte D, Jr, Kim JK, Gabel HW, Kamath RS, Mello CC, Ruvkun G (2005) *Nature* 436:593–597.
12. Dwyer ND, Adler CE, Crump JG, L'Etoile ND, Bargmann CI (2001) *Neuron* 31:277–287.
13. Hallam S, Singer E, Waring D, Jin Y (2000) *Development (Cambridge, UK)* 127:4239–4252.
14. Filipowicz W (2005) *Cell* 122:17–20.
15. Mello CC, Conte D, Jr (2004) *Nature* 431:338–342.
16. Simmer F, Tijsterman M, Parrish S, Koushika SP, Nonet ML, Fire A, Ahringer J, Plasterk RH (2002) *Curr Biol* 12:1317–1319.
17. Kennedy S, Wang D, Ruvkun G (2004) *Nature* 427:645–649.
18. Lehner B, Calixto A, Crombie C, Tischler J, Fortunato A, Chalfie M, Fraser AG (2006) *Genome Biol* 7:R4.
19. Sieburth D, Ch'ng Q, Dybbs M, Tavazoie M, Kennedy S, Wang D, Dupuy D, Rual JF, Hill DE, Vidal M, *et al*. (2005) *Nature* 436:510–517.
20. Chen Z, Han M (2001) *Curr Biol* 11:1874–1879.
21. Kim S, Wadsworth WG (2000) *Science* 288:150–154.
22. Hill E, Broadbent ID, Chothia C, Pettitt J (2001) *J Mol Biol* 305:1011–1024.
23. Down M, Power M, Smith SI, Ralston K, Spanevello M, Burns GF, Boyd AW (2005) *Gene Expr Patterns* 5:483–490.
24. Ciani L, Patel A, Allen ND, ffrench-Constant C (2003) *Mol Cell Biol* 23:3575–3582.
25. Hutter H (2003) *Development (Cambridge, UK)* 130:5307–5318.
26. Zhou Z, Hartwieg E, Horvitz HR (2001) *Cell* 104:43–56.
27. Lee J, Jongeward GD, Sternberg PW (1994) *Genes Dev* 8:60–73.
28. Korswagen HC, Coudreuse DY, Betist MC, van de Water S, Zivkovic D, Clevers HC (2002) *Genes Dev* 16:1291–1302.
29. Fradkin LG, Garriga G, Salinas PC, Thomas JB, Yu X, Zou Y (2005) *J Neurosci* 25:10376–10378.
30. Zou Y (2004) *Trends Neurosci* 27:528–532.
31. Pan CL, Howell JE, Clark SG, Hilliard M, Cordes S, Bargmann CI, Garriga G (2006) *Dev Cell* 10:367–377.
32. Hilliard MA, Bargmann CI (2006) *Dev Cell* 10:379–390.
33. Prasad BC, Clark SG (2006) *Development (Cambridge, UK)* 133:1757–1766.
34. Maduro M, Pilgrim D (1995) *Genetics* 141:977–988.
35. Hart AC, Sims S, Kaplan JM (1995) *Nature* 378:82–85.
36. Maricq AV, Peckol E, Driscoll M, Bargmann CI (1995) *Nature* 378:78–81.
37. McIntire SL, Reimer RJ, Schuske K, Edwards RH, Jorgensen EM (1997) *Nature* 389:870–876.
38. Colavita A, Krishna S, Zheng H, Padgett RW, Culotti JG (1998) *Science* 281:706–709.
39. Kamath RS, Martinez-Campos M, Zipperlen P, Fraser AG, Ahringer J (2001) *Genome Biol* 2:RESEARCH0002.